PERGAMON

Vision Research 38 (1998) 2135–2146

Vision Research

Spectral sensitivity of cones in the goldfish, *Carassius auratus*

Adrian G. Palacios [a], Francisco J. Varela [b], Ranjana Srivastava [a], Timothy H. Goldsmith [a,*]

[a] *KBT 736, Department of Molecular, Cellular, and Developmental Biology, Yale University, PO Box 208103, New Haven, CT 06520-8103, USA*
[b] *LENA–CNRS URA 654, Hopital de la Salpetriere, Paris, France*

Received 8 July 1997; received in revised form 29 September 1997

Abstract

The spectral sensitivities of retinal cones isolated from goldfish (*Carassius auratus*) retinas were measured in the range 277–737 nm by recording membrane photocurrents with suction pipette electrodes (SPE). Cones were identified with λ_{max} ($\pm$S.D.) at 623 ± 6.9 nm, 537 ± 4.7 nm, 447 ± 7.7 nm, and about 356 nm (three cells). Two cells (λ_{max} 572 and 576 nm) possibly represent genetic polymorphism. A single A_2 template fits the α-band of $P447_2$, $P537_2$, and $P623_2$. HPLC analysis showed 4% retinal:96% 3-dehydroretinal. Sensitivity at 280 nm is nearly half that at the λ_{max} in the visible. The λ_{max} of the β-band (in nm) is a linear function of the λ_{max} of the α-band and follows the same relation as found for A_1-based cone pigments of a cyprinid fish.

Keywords: Goldfish; *Carassius*; Cones; Dehydroretinal; Spectral sensitivity; Visual pigment template spectra; Porphyropsin; Photocurrents

1. Introduction

One purpose of the present work is to characterize the spectral sensitivities of goldfish cones. Recent behavioral work indicates that the goldfish *Carassius auratus* has tetrachromatic color vision [1–3]. The goldfish retina has several forms of single as well as double cones [4–6], and four spectral classes of cones have been identified by microspectrophotometry (MSP) with λ_{max} in the red, green, blue, and UV regions of the spectrum [7,8]. Four spectral classes of cones, including a UV receptor, have been described in at least 16 other species of fish representing four families (MSP: [3,9]; spectral sensitivity of single cones: [10]). Compared with some other fish, however, the goldfish has very few UV cones [8].

Johnson et al. [11] sequenced five opsin genes from goldfish: rod opsin and four cone pigments. In addition to the opsin of the blue-sensitive cone and a putative polymorphic variant of the red cone, they found opsins associated with two green-sensitive cones (Gfgr-1 and Gfgr-2) homologous to chicken green [12], a cone pigment of birds that has evolutionary affinities to rod opsin. The molecular genetic evidence for polymorphism is not yet reconciled with MSP. The gene for the UV-sensitive pigment has also been sequenced [13]. It is homologous to the violet receptor of humans and chickens and is expressed in small, single cones.

The goldfish utilizes 3-dehydroretinal in the chromophore of its visual pigments, and this provides a second incentive for the present experiments. Dartnall [14] suggested that the spectra of A_1-based visual pigments have a constant shape when plotted as a function of wave number. This turned out to be an approximation, as half-bandwidth (in units of $1/\lambda$) varies with λ_{max} [9,15]. Many visual pigments have a common bandwidth, however, when absorbance is plotted on a normalized frequency axis (i.e. λ_{max}/λ; [10,16–20]). Spectral sensitivity measurements of individual photoreceptors characteristically extend to long wavelengths where absorbance is too low to be measured, and in such data log sensitivity falls linearly when plotted as a function of λ_{max}/λ [18,19]. The spectral shapes of many visual pigments are therefore described by a common template in λ_{max}/λ, but as $retinal_1$-based amphibian rods are somewhat narrower [20] and UV fish cones narrower still [10], further work is required to establish the extent of variation, the relative position of

* Fax: +1 203 4323494; e-mail: timothy.goldsmith@yale.edu.

0042-6989/98/$19.00
PII: S0042-6989(97)00411-2

the β-band, and the slope of the long-wavelength tail. In the present experiments we have used suction pipette electrodes (SPE) to measure the spectral sensitivities of isolated goldfish cones containing a preponderance of 3-dehydroretinal. The α, β, and γ absorption bands of the visual pigments were fit to a dehydroretinal-based (retinal$_2$-based) template consisting of the sum of three log-normal functions, following the method of Stavenga et al. [18]. This procedure yields an estimate of the spectral position of the β-band, information not so reliably acquired by MSP. An alternative α-band template for retinal$_2$-based visual pigments that extends to long wavelengths is also presented and compared with the shape of retinal$_1$-based spectral sensitivity [19]. A preliminary report of this work has been published in abstract (see Ref. [21]).

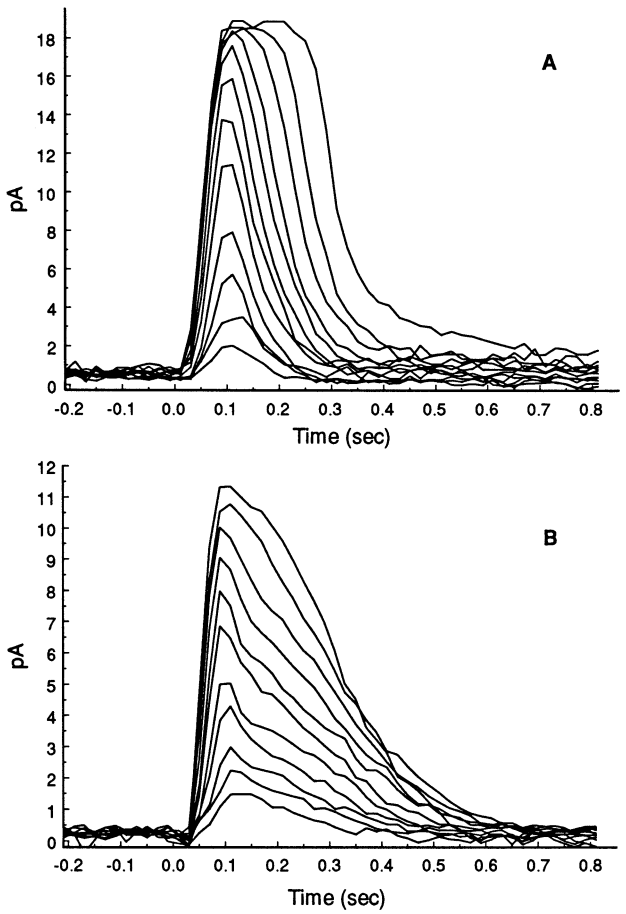

Fig. 1. (A): A cell maximally sensitive at 537 nm. The corresponding photon flux (and trae numbers) are: 150(5); 240(6); 600(3); 950(2); 1500(2); 2390(2); 3780(2); 5990(2); 9500(2); 15000(2); 30100(1); and 60200(2). (B): A blue-sensitive cone with λ_{max} at 447 nm. The number of photons μm^{-2} $flash^{-1}$ (and the number of responses averaged in each trace) are: 410(3); 650(6); 820(4); 1300(4); 2060(3); 3270(3); 5200(3); 80200(3); 13000(3); 20600(3); 26000(1).

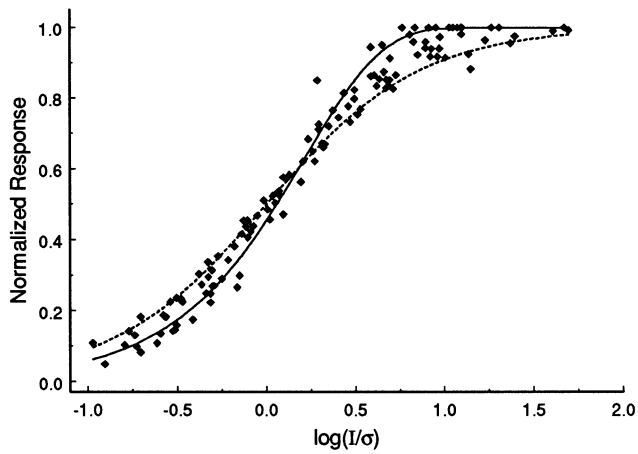

Fig. 2. Response-amplitude function of 14 cones from three spectral classes. The broken curve is normalized photocurrent as a function of $I/(I+\sigma)$, where σ is the intensity (I) for a half-maximal response. Solid curve is normalized response as a function of $1-\exp(-k_f I)$, where $k_f = \ln(2)/\sigma$. To facilitate comparison, individual values of σ were measured for each cell and the data plotted on a normalized abscissa (log I/σ).

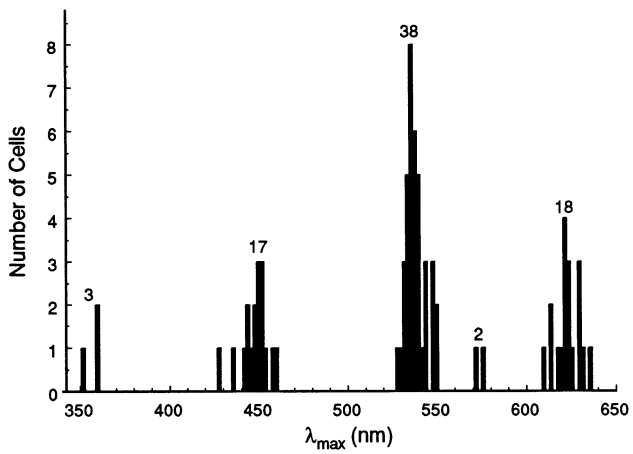

Fig. 3. Spectral classes of 78 goldfish cones. UV cones are uncommon in *Carassius auratus*.

2. Methods

2.1. Animals

Goldfish, *Carassius auratus*, 5–9 cm body length, were a gift from Ekk Will Wildlife Resources (Gibsonton, FL). They were maintained in a fresh-water aquarium at 22°C on a 14/10 light/dark cycle, and fed dry food (Tetra). The animals were kept for several weeks before they were used for experiments.

Table 1
Cellular identity and spectral class (λ_{max}) for 64 goldfish cones

	623 nm	537 nm	447 nm	UV	574 nm
Single	3	10	18	3	1
Long double	10	0	0	0	1
Short double	0	18	0	0	0

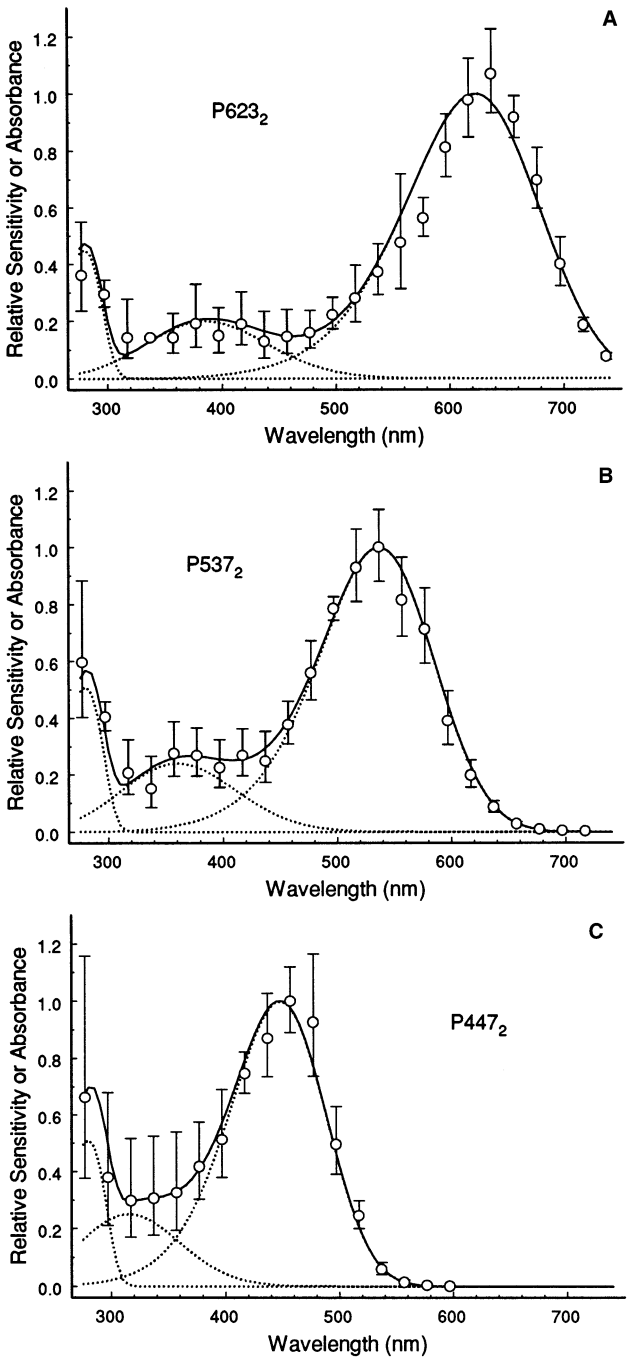

Fig. 4. The spectral sensitivities of the 623, 537, and 447 nm cones (solid curves) can be described as the sum of three log-normal functions (broken curves) for the α, β, and γ absorption bands of the visual pigments (anti-log transform of Eq. (1), [18]). This analysis provides an estimate of the spectral position of the β-band. See the text for details of the curve-fitting. In this figure error bars are asymmetrical and differ greatly in size because experimental variation in log sensitivity is approximately normally distributed [10].

2.2. Preparation of the tissue

Following 2–3 hours of dark adaptation, an animal was anesthetized (0.05% 3-amino benzoic acid ethyl ester, MS222, Sigma, St. Louis, MO) and decapitated.

Table 2
Template coefficients for dehydroretinal-based visual pigments

Equation 1	α-band	β-band	γ-band	Equation 2	α-band
c_0	304	140	647	a	70
c_1	5.01	1.52	23.4	A	0.86
c_2	9.4	0.87	205.34	b	29
				B	0.91
				c	−17.9
				C	1.118
				D	0.806

The eyes were removed under dim red light and the retinas isolated under infrared illumination. One was used immediately and the other maintained in darkness at 4°C in L-15 medium (Gibco, Gaithersburg, MD) for 12–24 hours before recording. To measure photocurrents, exposed outer segments in finely chopped pieces of retina were drawn into suction pipette electrodes. The recording chamber was superfused with physiological saline containing (in mM): NaCl, 102; KCl, 2.6; $MgCl_2$, 1; $CaCl_2$, 1; glucose, 5; $NaHCO_3$, 28 at pH 7.8–8.0 [22]. Temperature was 22°C.

2.3. Optical system

A 150W xenon arc lamp, operated from a stabilized power supply (Ealing, Holliston, MA), and a monochromator (600 lines mm^{-1} grating, Bausch and Lomb, Rochester, NY) were used to isolate narrow wavelength bands (6 nm half bandwidth) from 277 to 737 nm. An electronic shutter (Uniblitz, Vincent Associates, Rochester, NY) controlled the duration of the flash. A pair of optical wedges consisting of graded metallic films deposited on counter-rotating quartz

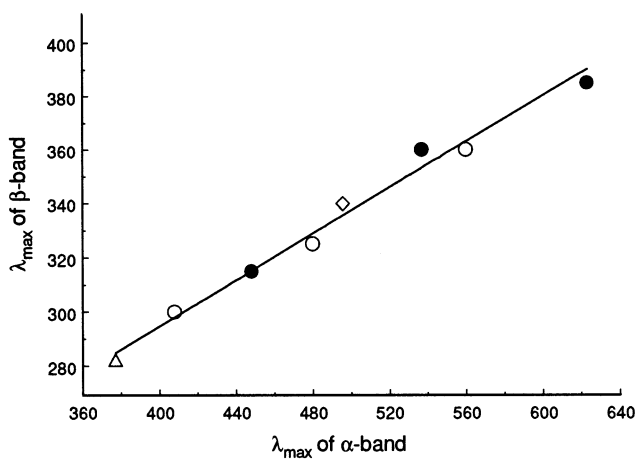

Fig. 5. Spectral position (λ_{max}) of the β-band as a function of the λ_{max} of the α-band for several visual pigments. Filled circles: retinal$_2$-based cone pigments of the goldfish (*Carassius auratus*, present work). Open circles: retinal$_1$-based cone pigments of another teleost, the giant danio (*Danio aequipinatus*, [10]). Open diamond: cattle rhodopsin [18]. Open triangle: 11-*cis* retinal [51].

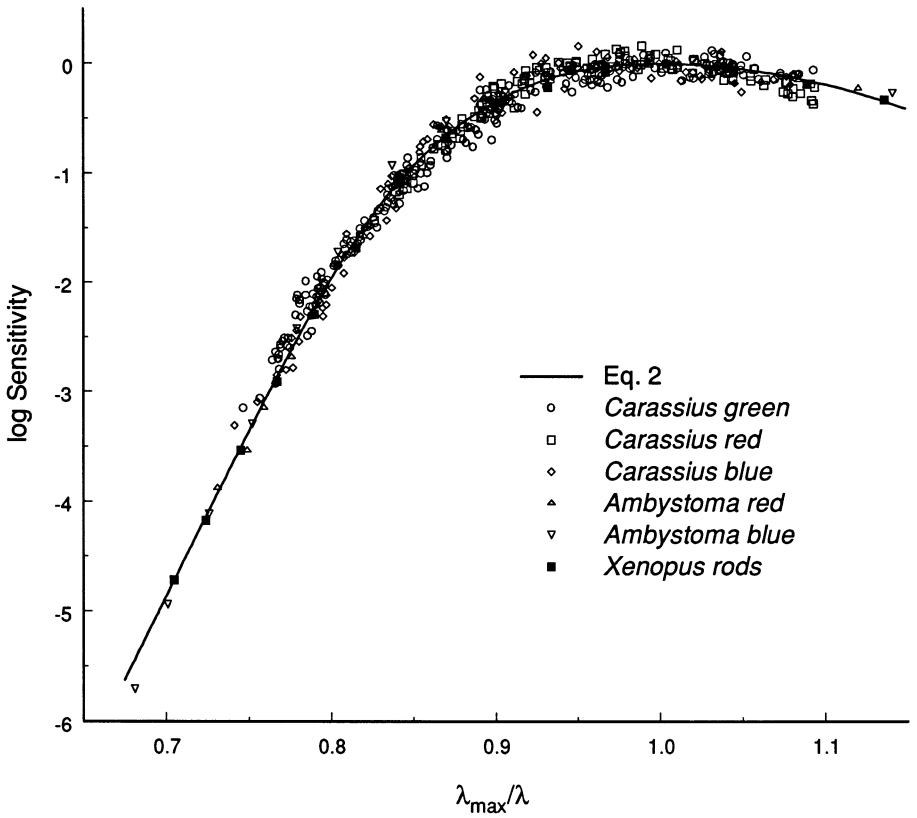

Fig. 6. Pooled data for the spectral sensitivity of vertebrate photoreceptors containing 3-dehydroretinal-based visual pigments, plotted as a function of normalized frequency. The data are fit by a single function (Eq. (2), coefficients in Table 2) of the form introduced by [19] to describe mammalian rhodopsins. See the Methods for details of the analysis. The data consist of 69 *Carassius* cones of three spectral classes (present work), 28 red and 5 blue *Ambystoma* cones [33], and 11 *Xenopus* rods [20].

discs were used to control the intensity of the stimulus beam. The stimulus was plane-polarized perpendicular to the long axis of the outer segment (Polaroid HNP'B, Norwood, MA; ca. 17% transmission at 280 nm). Long-pass filters (#24 and #29, Kodak Wratten, Rochester, NY; CS2-64, Corning Inc., Corning, NY; GG400, GG475, Schott, Mainz, Germany) removed stray light and the second-order spectrum. For wavelengths <360 nm a short-pass filter (UG11, Schott, Mainz, Germany) suppressed stray light at longer wavelengths. A second lamp source with two infrared transmitting filters (optical density >8 at wavelengths shorter than 750 nm) and an IR-sensitive video camera were used to monitor the preparation during experiments. Lamp calibration was accomplished with a calibrated photodiode (UV100, United Detector Technology Sensors, Hawthorne, CA).

2.4. Recording

Photocurrents from individual outer segments of cones from 16 fish were measured using Ag/AgCl electrodes and a PC-501A patch cell amplifier (Headstage 5101-10, Warner Instrument Corp., Hamden, CT). Before A/D conversion (DAS-8/AO, 12-bit resolution, Metrabyte, Keithley, Taunton, MA) the high frequencies were removed with an active, 20 Hz low-pass, 4-pole Bessel filter (Frequency Devices, Haverhill, MA). Time to peak was corrected for the 20 ms delay introduced by this filter. Wedges, monochromator, and shutter were controlled by a computer, and data were saved on the hard drive for later analysis.

2.5. Integration time

The integration time was determined from

$$t_{\mathrm{i}} = \frac{\int r(t)dt}{r_{\mathrm{peak}}}$$

where $r(t)$ is the response to a dim flash and r_{peak} is the peak amplitude [23].

2.6. Sensitivity to dim flashes

The responses of individual cones to 10 ms flashes in the linear range of the response-amplitude function were smoothed with a three-point running average, and the peak amplitude of the response, r_{peak} calculated from the average of 5–6 responses. The sensitivity to a dim flashes (S_{df}) was defined as

$S_{df} = r_{peak}/i$,

where i is the intensity in photons flash^{-1} μm^{-2} and r_{peak} is in pA.

2.7. Analysis of spectral sensitivity data

Spectral sensitivity of individual cells (log S_{df} vs λ) was first normalized and the upper 0.5 log unit of the α-band fit to a provisional log-normal template of the form

$$\log[\alpha(\lambda)] = \log\{\exp[c_0 x^2(1 + c_1 x + c_2 x^2)]\} + \log(k) \quad (1)$$

where $x = \log(\lambda/\lambda_{max})$ [18] and $\alpha(\lambda)$ is relative absorbance of the α-band of the visual pigment. At this stage of the analysis we used the coefficients appropriate for porphyropsin ($c_0 \ldots c_2$) based on Bridges' [24] spectrum of rod porphyropsin [18] and found for each cell the minimal least-squares fit, with λ_{max} and $\log(k)$ as free parameters. The spectral sensitivity data for each cell were then shifted vertically by $\log(k)$ so as to collapse the cell-to-cell variation in absolute sensitivity, and spectral sensitivity of each cell was plotted as a function of (its) λ_{max}/λ to capture a common bandwidth, thus compensating for any possible polymorphism in λ_{max} within the spectral class being analyzed.

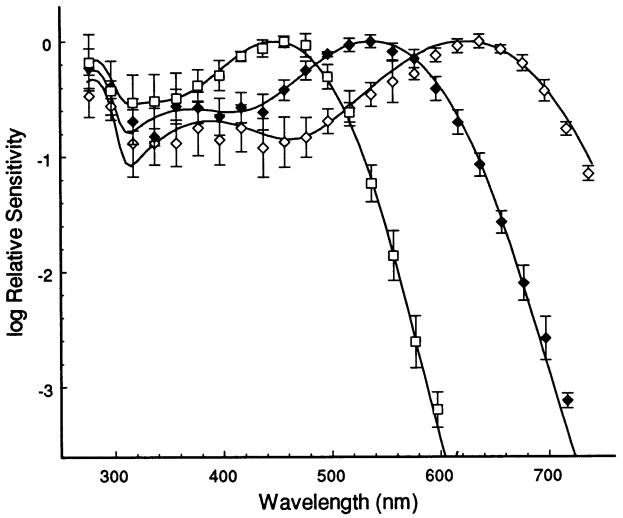

Fig. 7. Three spectral classes of goldfish cones found in the highest numbers, plotted as log sensitivity ±1 S.D. At short wavelengths the curves are the logs of the solid curves in Fig. 4 and are calculated from Eq. (1); through the peak of the α-absorption band they follow Eq. (2), as in Fig. 6. The two templates overlap extensively over the top of the α-band.

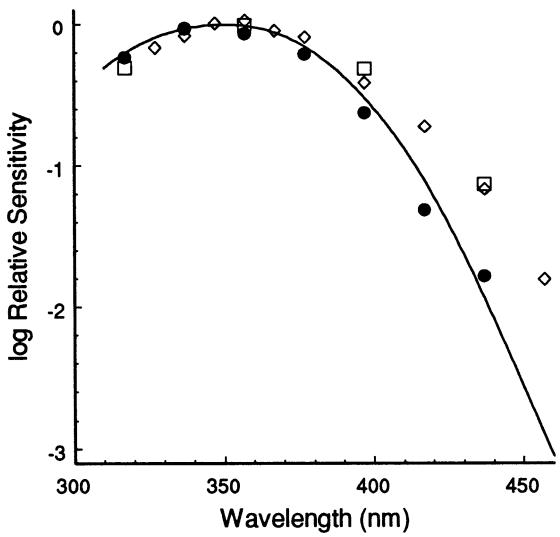

Fig. 8. Spectral sensitivity of three UV cones from goldfish. One is adequately described by the retianl$_2$-based template; the other two are substantially broader.

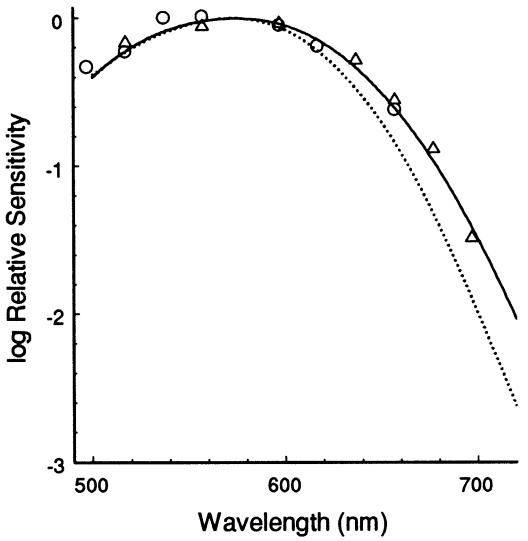

Fig. 9. Two cones with λ_{max} at 574 ± 2 nm that did not belong to any of the major spectral classes. Solid curve: template for dehydroretinal-based pigments (Fig. 6). Dotted curve: equivalent template for retinal-based pigments [19,10].

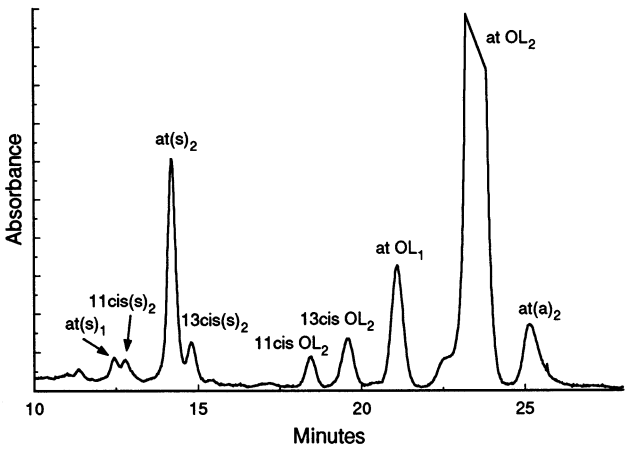

Fig. 10. HPLC separation of retinols and retinal oximes extracted from light-adapted goldfish eyes (retina and pigment epithelium combined). There was about 30 times as much free alcohol as aldehyde, and the all-*trans* 3-dehydroretinol peak (at OL_2) goes off scale in this figure. 3-Dehydroretinal accounted for 96% of the oxime peaks and 3-dehydroretinol about 88% of the alcohols (molar basis). Symbols: at = all-*trans*; (s) = *syn* forms of the oximes; (a) = *anti* forms of the oximes; OL = alcohols; subscripts = A_1 or A_2 derivatives. Normal phase silica column developed with 7% dioxane in hexane at a flow rate of 1ml min^{-1}.

Table 3
Cone pigments of *Carassius auratus* ($\lambda_{max} \pm$ S.D., nm)

UV	Short	Middle	Long	Authors	Method
356	447 ± 7.7	537 ± 4.7	623 ± 6.9	present work	SPE
360	452 ± 1.4	532 ± 1.9	614 ± 4.9	Bowmaker et al. [8]	MSP
	453	53 3	620	Hárosi [46]	Reanalysis
	455 ± 3	530 ± 3	625 ± 5	Hárosi and MacNichol [7]	MSP
	455 ± 3	535 ± 3	620 ± 3	Liebman and Entine [48], Liebman [49]	MSP
	445 ± 15	530 ± 5	625 ± 5	Marks, [50]	MSP

SPE, suction pipette electrode; MSP, microspectrophotometry

The next step was to refine the fit of Eq. (1) to the entire (replotted) set of spectral sensitivity data by finding the minimal least squares values for c_0 and c_1. (The value of c_2 is not an independent parameter as it is given by $3c_1^2/8$.) Finally, the λ_{max} of each cell was recalculated by finding the best fit to this modified template. Values of λ_{max} obtained in this iteration were averaged to characterize each spectral class.

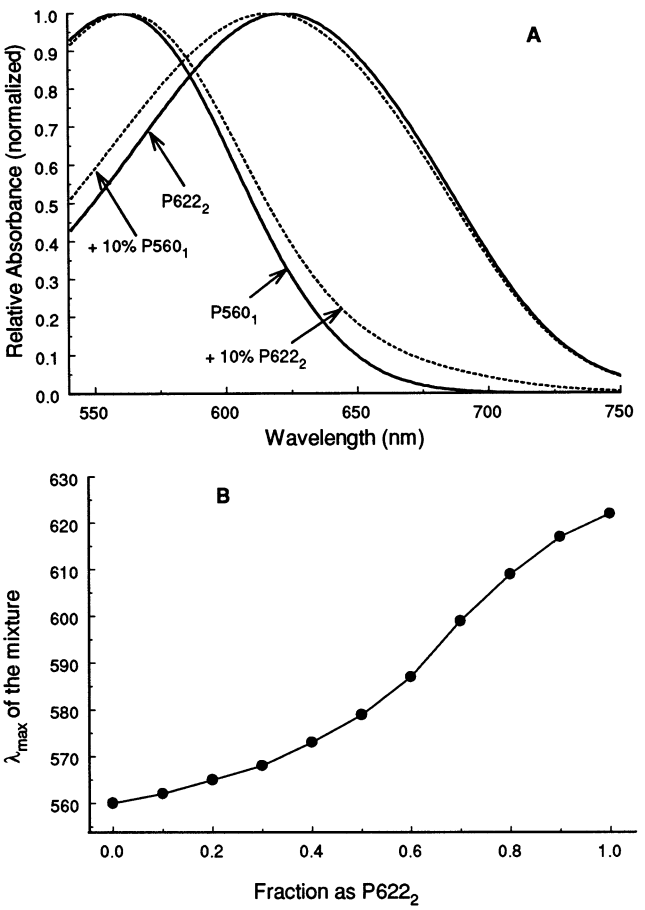

Fig. 11. (A): Normalized template spectra for $P560_1$ and $P622_2$ pigment pairs (solid curves) and when each is contaminated with a 10% (by absorbance) mixture of the other (dotted curves). The presence of a small amount of a $retinal_1$-based pigment has virtually no effect on the shape of the absorbance spectrum of a $retinal_2$ pigment at long wavelengths and would be difficult to detect by MSP or spectral sensitivity measurements. (B): Variation of λ_{max} of the pigment mixture as a function of the mole fraction as $P522_2$.

This log-normal template provides a convenient way of characterizing the shape of the α-band around the λ_{max}, but it does not extrapolate well at long wavelengths where log sensitivity falls linearly. A linear regression of log sensitivity on λ_{max}/λ must therefore be matched to the log-normal template where their slopes are the same. Lamb [19] has proposed an alternative template that combines these features of the α-band absorption in a single function:

$$\log\alpha(\lambda) = \log\frac{1}{\exp\left[a\left(A-\frac{\lambda_{max}}{\lambda}\right)\right]+\exp\left[b\left(B-\frac{\lambda_{max}}{\lambda}\right)\right]+\exp\left[c\left(C-\frac{\lambda_{max}}{\lambda}\right)\right]+D} \quad (2)$$

In order to find coefficients appropriate for photoreceptors containing dehydroretinal-based pigments, the four terms in the denominator of Eq. (2) were manipulated independently while using an interactive graphics program to find an optimal fit of Eq. (2). The long-wavelength tail was fit while viewing a linear regression of log sensitivity on λ_{max}/λ; the top of the curve was fit to a plot of Eq. (1) while viewing as $\alpha(\lambda)$ rather than $\log[\alpha(\lambda)]$. This procedure produces an agreement of the two templates (Eqs. (1) and (2)) within their region of overlap that is within the resolution of the computer's monitor and is sufficient for all practical purposes.

An advantageous feature of the treatment of Stavenga et al. [18] is that the α, β and γ bands can be fit to data independently of one another. By plotting the data as sensitivity rather than log sensitivity, acceptable fits of log normal functions for the β and γ bands were found by eye.

2.8. Identification of chromophores

Several light-adapted eyes were frozen and the retinoids later extracted [25]. Retinols and retinaldeydes were separated on a normal-phase silica column (Rainin Microsorb, Woburn, MA; 5 μm) developed with 9 or 7% dioxane in hexane at a flow rate of 1 ml min^{-1} [26]. Retinyl esters in these eyes were not analyzed. Retinoids were detected by measuring spectral absorbance at 357 nm. To assist in identification of

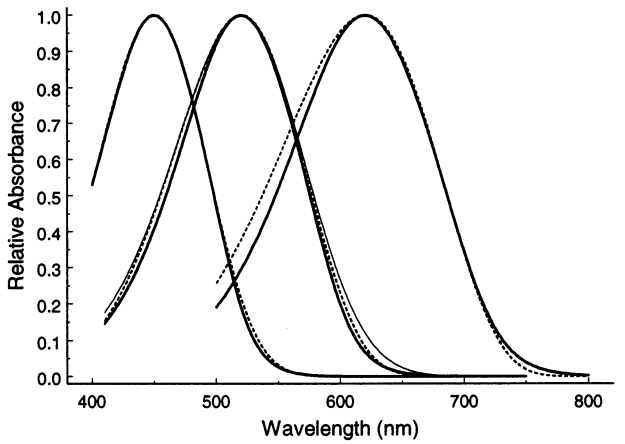

Fig. 12. Comparison of the most recent templates for the α-band of dehydroretinal visual pigments. Heavy curves: based on spectral sensitivity of goldfish cones (present work). Thin solid curve: from Ref. [18] and based on Ref. [24] extracts of porphyropsin from fish rods. Both templates utilize Eq. (2), but optimal fit to Bridges' [24] data required a slightly broader bandwidth. Dashed curves: from Mooij and van den Berg [45] and based on Hárosi's [46] MSP of goldfish cones.

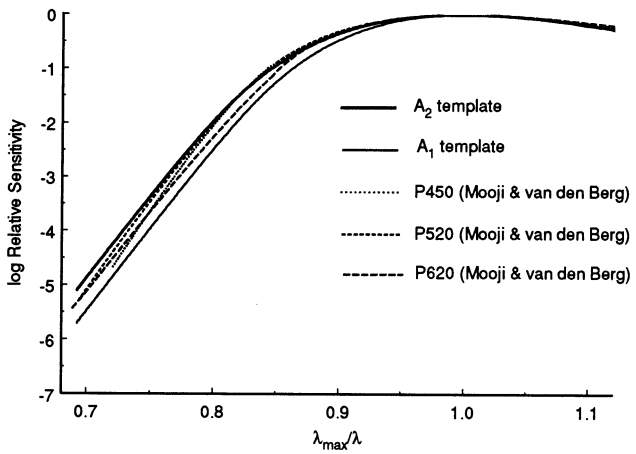

Fig. 13. Templates for spectral sensitivity of cones containing dehydroretinal-based visual pigments. Heavy solid curve: retinal$_2$ template from the present work (Fig. 6 and Eq. (2)). Thin solid curve: retinal$_1$ template [19]. These retinal$_1$ and retinal$_2$ templates have very similar slopes at long wavelengths. Broken curves: calculated from the equations of Mooij and van den Berg [45]. The log-normal function of Mooij and van den Berg [45] does not employ normalized frequency as the independent variable, and their three curves are thus all slightly different. (Furthermore there appears to be an error in their Table 4 in that the coefficients for their α_0 and α_1 for λ_0 are inconsistent with their Table 3 and their values of λ_{max}. We re-computed them to be -14.8066 and 1.1395 prior to calculating their modified Lewis function.)

retinal and retinol, the solution from the column flowed from the absorbance detector to a fluorimeter. Fluorescence was activated by a broad band of near UV light with maximum energy at 330 nm and measured with a detector shielded from wavelengths shorter than 500 nm. Retention times and (for retinol) ratios of absorbance to fluorescence were compared to standards of known isomeric composition, made from all-*trans* retinal (Sigma, St. Louis, MO) and all-*trans* 3-dehydroretinal (F. Hoffmann-La Roche, Basel, Switzerland). All-*trans* 3-dehydroretinol was made by reducing an aliquot of the aldehyde with sodium borohydride in ethanol. Amounts were quantified by measuring peak areas with integration software (Perkin Elmer Nelson Systems, Cupertino, CA) and comparing with standards of known concentration. Mixtures of A_1 and A_2 standards were cochromatographed with aliquots of retinal oximes and retinols in order to facilitate identification.

3. Results

3.1. Photocurrent responses

Representative photocurrent responses to 10 ms monochromatic flashes of increasing intensity are shown in Fig. 1. For a subset of the green-sensitive cones (the class for which the sample size was the largest), time-to-peak was 157 ± 39 ms ($n = 9$) and the integration time was 171 ± 52 ms. In some cones, membrane capacitance slows the responses [27,28], and accurate measurements of the kinetics of photocurrents requires that the cell be voltage-clamped. These cells were not voltage-clamped, and this time-to-peak may thus be over-estimated.

Fig. 2 shows the normalized amplitude of response as a function of the log of the photon flux for 14 cones of the three principal spectral classes (three blue, six green, and five red). The solid curve follows $r/r_{max} = 1 - \exp(-k_f I)$ [29]; the dashed curve is $r/r_{max} = I/(I + \sigma)$, where σ is the intensity for a half-maximal response [30]. Each cell was plotted with its own value of $\sigma[= \ln(2)/k_f]$. From the available data it is not clear that one of these expressions provides a consistently better fit than the other.

3.2. Variation in λ_{max}

The procedure for assigning values of λ_{max} to each cell is described in Section 2. Most of the cells were in one of three clusters, with λ_{max} at 447 ± 7.7, 537 ± 4.7, and 623 ± 7.9 nm (mean $\pm$ S.D.) (Fig. 3). Five cells had λ_{max} that did not fall in any of the three major clusters. Three were in the near UV and two had λ_{max} at 572 and 576 nm, approximately midway between the red- and green-sensitive clusters (Fig. 3). These outliers will be considered below.

According to Walls [31], two types of paired cones are found in teleosts, referred to as twin cones and double cones. The two members of double cones differ in size, but the asymmetry is not as pronounced as in the double cones of birds and reptiles. Engström [32]

Table 4
Average values of log sensitivity ± 1 S.D. at different wavelengths for three classes of goldfish cones; the chromophore was dehydroretinal; the number of cells in each average is given in the column labeled *n*

λ	623 nm			537 nm			447 nm		
	log *S*	S.D.	*n*	log *S*	S.D.	*n*	log*S*	S.D.	*n*
277	−0.47	0.184	9	−0.23	0.171	27	−0.18	0.244	12
297	−0.56	0.070	3	−0.39	0.055	5	−0.42	0.255	5
317	−0.88	0.292	10	−0.69	0.196	31	−0.53	0.242	14
337	−0.88	0.018	7	−0.82	0.247	8	−0.52	0.236	6
357	−0.88	0.203	15	−0.56	0.149	33	−0.49	0.222	15
377	−0.75	0.238	7	−0.57	0.136	9	−0.38	0.140	6
397	−0.85	0.218	16	−0.65	0.160	34	−0.29	0.130	15
417	−0.75	0.204	6	−0.57	0.132	8	−0.13	0.042	6
437	−0.92	0.257	16	−0.61	0.155	34	−0.06	0.073	15
457	−0.87	0.218	6	−0.42	0.087	8	0.00	0.050	8
477	−0.83	0.173	16	−0.25	0.080	34	−0.03	0.100	15
497	−0.69	0.108	8	−0.11	0.023	10	−0.30	0.104	10
517	−0.58	0.152	16	−0.03	0.059	34	−0.61	0.084	15
537	−0.46	0.104	9	0.00	0.055	15	−1.23	0.158	11
557	−0.35	0.180	16	−0.09	0.073	34	−1.86	0.217	15
577	−0.28	0.053	12	−0.15	0.080	11	−2.61	0.224	8
597	−0.12	0.059	15	−0.41	0.105	34	−3.19	0.153	2
617	−0.04	0.061	14	−0.70	0.104	16			
637	0.00	0.059	17	−1.07	0.100	34			
657	−0.07	0.035	13	−1.57	0.096	19			
677	−0.19	0.067	17	−2.10	0.151	32			
697	−0.43	0.093	17	−2.58	0.189	18			
717	−0.76	0.058	10	−3.12	0.063	2			
737	−1.15	0.064	10						

reviewed the distribution of cone types in a variety of teleosts. Goldfish retinas contain double cones and several subclasses of single cones [4]. The identity of 64 of the cells for which we obtained spectral data are listed in Table 1. These results are consistent with earlier reports [7,8]. In the present work we have not tried to identify subclasses of single cones.

3.3. α-, β- and γ-bands of the three principal spectral classes

Fig. 4 shows the spectral sensitivities of the 623, 537, and 447 nm cones along with log-normal template functions for the α, β, and, γ bands (Eq. (1); [18]). For the analysis of Fig. 4, cells were included only if their λ_{max} fell within 2 S.D. of the mean. One cell in the 447 nm group, two in the 537 nm cluster, and one in the 623 nm group were omitted by this criterion.

As described in Section 2, the α-band function was obtained as part of the procedure for determining the λ_{max}. The β- and γ-band functions were fit by eye, so that the sum of the three curves followed the data points. To achieve this fit, the peak heights of the β- and γ-bands and the λ_{max} of the β-band were varied. The same band-width coefficient for the β-band was used for all three pigments. Bandwidth and λ_{max} for the γ-band were assumed the same as for A_1 pigments [18]. All the coefficients are summarized in Table 2.

The λ_{max} of the β-band is found at longer wavelengths as the spectral position of the α-band moves toward the red. (Fig. 5). The data from retinal$_1$- and retinal$_2$-based pigments follow the same relationship, in which the λ_{max} of the β-band (in nm) is a linear function of the λ_{max} of the α-band: $\beta_{\lambda max} = 0.429\alpha_{\lambda max} + 123$.

3.4. An α-band template for log sensitivity

In order to determine the shape of the template spectrum at long wavelengths, we have fit Eq. (2) to a combined data set consisting of 69 goldfish cones from these three spectral classes, 11 *Xenopus* rods [20], and 33 *Ambystoma* cones from two spectral classes ([33], see Fig. 3). Some of Makino and Dodd's *Ambystoma* cones appear to have contained mixtures of retinal and dehydroretinal; consequently for the present purposes we have used only the most red-shifted cones. In order to assign values of λ_{max} to the *Ambystoma* data, average values of log sensitivity for two cone classes were fit by eye to the goldfish template described by Eq. (1): 606 nm for the 28 red-sensitive cones and 435 nm for 5 blue-sensitive cells.

The resulting template based on these three sources of data is shown in Fig. 6, and the coefficients for the template are given in Table 2. This template curve is valid for values of $\lambda_{max}/\gamma < 1.1$. The overlap with the

template based on Eq. (1) is within 0.02 log units for $0.8 < \lambda_{max}/\gamma < 1.1$.

The spectral sensitivities of the three major spectral classes of goldfish cone are summarized in Fig. 7, with the S.D. in log sensitivity. At long wavelengths the curves follow the template in Fig. 6, but at short wavelengths they are the logarithmic transforms of the solid curves in Fig. 4. Average data with S.D. are given in the Appendix (see Table 4).

3.5. UV cones

Three cones were found with maximum sensitivity in the near UV (Fig. 8). One of these (filled symbols, λ_{max} at 350 nm) was reasonably well fit by the template for dehydroretinal-based pigments that appears in Fig. 6. The spectral sensitivity of the other two cells (open symbols, λ_{max} at 359 nm) was substantially broader.

3.6. Two cells with λ_{max} at 574 nm

Two cells with λ_{max} at about 574 nm were clearly different from the major spectral classes (Fig. 3). Their spectral sensitivities (Fig. 9), however, are well fit by the retinal$_2$-based template and are distinctly broader than the A_1 template based on cones from *Danio aequapinnatus* [10]. It therefore seems unlikely that their visual pigments used retinal rather than dehydroretinal, and a possible explanation for their λ_{max} is that they contained a different opsin. The two cells were found in different retinas. One retina also contained cones from all three principal classes; the other yielded a red-sensitive cone.

3.7. Analysis of retinoids

Several eyes from fish that were used for spectral recording were frozen and their retinoids later extracted and analyzed by HPLC (Fig. 10). These light-adapted eyes contained a preponderance of 3-dehydroretinoids: 96% of the aldehyde and 88% of the free alcohol. There was about 30 times more free alcohol than aldehyde. Retinyl esters were not examined in these eyes.

4. Discussion

4.1. Comparison with earlier work on different spectral cone classes

The spectral sensitivity of goldfish cones has been measured by MSP in several laboratories. This work is summarized and compared with the present findings in Table 3. The results are generally in good agreement in showing three main classes of cones absorbing maximally in the visible region of the spectrum.

Goldfish UV receptors are few and therefore difficult to find. They may be fewer in larger, older fish [8,34] as they are in salmonids [35,36]. Two of the three UV receptors that we have found in this study (Fig. 8) have unexpectedly broad spectral sensitivity. On the basis of similar sensitivity measurements, Makino and Dodd [33], found that the UV cones of tiger salamanders (*Ambystoma tigrinum*) contain what appears to be small but variable amounts of two other opsins. Similarly, goldfish UV cones might express minor amounts of at least one other visual pigment. Alternatively, the Schiff's base linkage of the chromophore might exist in a mixture of protonated and unprotonated forms [9]. The evidence for this idea is equivocal [10], but an unprotonated Schiff's base offers the intriguing possibility of accounting for the very short wavelength absorption of UV visual pigments [9]. In the A_1-based system of *Danio aequipinnatus* [10] there was no convincing evidence for a second pigment, and the λ_{max}/λ template for UV cones was narrower than the single template spectrum that fits fish and primate cones with λ_{max} in the visible region of the spectrum. The template for dehydroretinal-based UV pigments may also be narrower than the curve in Fig. 8 if all three of the UV cones in this study contained more than one pigment.

There were two cells with λ_{max} at about 574 nm that did not fall into any of the other spectral classes. As shown in Fig. 9 (see also below), the width of the α-band is not consistent with an A_1-chromophore in association with the opsin of the 623 nm pigment. The small number of cells may indicate a relatively uncommon allele in a system of genetic polymorphism, although one of the cells was accompanied in the same retina by cones from both the long- and middle-wavelength spectral classes. Suggestive evidence for polymorphism comes from another source. In a study of cloned sequences of goldfish opsins, Johnson et al. [11] were unable to find the long-wavelength pigment, but they did report an opsin that forms a 525 nm pigment when regenerated with 11-*cis* retinal. Using empirical formulas for relating the λ_{max} of A_1/A_2 pigment pairs, if coupled to 11-*cis* dehydroretinal, this opsin should have λ_{max} at 566 nm [37] or 563 nm [9]. Johnson et al. [11] attribute this opsin to a polymorphic variant, and it is possible that it corresponds to the 574 pigment in the two cones we have found. The published MSP data on goldfish and carp, however, provide no evidence of opsin polymorphism.

Johnson et al. [11] found two genes they believe correspond to the green-sensitive pigment. When combined with retinal (rather than dehydroretinal) their values of λ_{max} were at 505 and 511 nm. The calculated retinal$_2$-based pigments should have λ_{max} at 537 and 546 nm [37] or 532 and 541 nm [9]. The distribution of λ_{max} of the 537 nm cones in Fig. 3 is broad enough to embrace two pigments with similar λ_{max}, but without a

much larger sample it is hard to make a convincing case that more than one spectral type is present in this population.

4.2. Sensitivity of the γ-band

All three of the cones that absorb maximally in the visible region of the spectrum are sensitive to light absorbed by aromatic amino acids in the opsin moiety of the visual pigment (Fig. 4). The average ratio of sensitivity at 280 nm to sensitivity at the λ_{max} in the visible ranged from about 0.37 to 0.67, but the differences between receptor classes were not statistically significant. A similar result was found for the A_1-based cone pigments in *Danio aequipinnatus*, [10]. This sensitivity of the γ-band appears much too great to be accounted for by fluorescence and is likely due to intramolecular energy transfer, as found by Kropf [38] for the bleaching of rhodopsin in solution [10,20].

4.3. Presence of both retinal and dehydroretinal in goldfish

Although at one time the visual system of *Carassius* was thought to utilize 3-dehydroretinal exclusively, when obtained from commercial suppliers the retinas of these fish ordinarily contain variable amounts of both rhodopsin and porphyropsin. Partial bleaching of detergent extracts shows up to 15% rhodopsin, and the proportion can be greatly increased by lengthening photoperiod and elevating temperature [39–41]. The finding that the fish used in the present study contained only a few per cent retinal supports the premise that the spectral sensitivity curves reflect dehydroretinal-based visual pigments.

In order to explore how spectral sensitivity should be changed by the presence of small amounts of one chromophore in the presence of the other, the templates for retinal$_1$- and retinal$_2$-based pigments were used to calculate the absorption spectra of mixtures (Fig. 11). Contamination should be most readily detected when there is the largest difference between the λ_{max} of the members of a pigment pair, and for this calculation we therefore assumed $\lambda_{max} = 560$ nm for the retinal$_1$ pigment and 622 nm for the retinal$_2$ pigment. The presence of 10% of P560$_1$ in the presence of a preponderance of P622$_2$ has the largest effect at short wavelengths, and the long wavelength tail of absorption is so little affected that it would not be detectable in usual measurements of spectral sensitivity. The converse is not true, however. A small proportion of a retinal$_2$ pigment in the presence of retinal$_1$ pigment should be more readily detected by its effect at long wavelengths (Fig. 11(A)). The λ_{max} of the mixture shifts non-linearly with the proportion of P622$_2$ (Fig. 11(B)).

These effects are evident in published data. Some spectra of red-sensitive cones, like that in Fig. 4(A), descend to a minimum around 470 mm that is about 20% the value at the λ_{max} [42,43]. Others show the effects of mixtures of A_1 and A_2 chromophore, in which the λ_{max} is shifted to shorter wavelengths from 622 nm and absorption is elevated around 460–480 nm [8,40].

4.4. Template spectra for dehydroretinal-based visual pigments

As discussed in Section 1, since Mansfield [16] and MacNichol [17] first suggested that the spectra of visual pigments have a constant shape when plotted as a function of normalized frequency, several mathematical templates have been constructed that are valid over a wide range of λ_{max}. Although with limited (or no) theoretical basis, such templates are nevertheless very useful in characterizing noisy MSP data or spectral sensitivity measurements made from single cells at widely separated wavelengths. As we have used it here, the formulation of Stavenga et al. [18] is particularly useful in finding the λ_{max} of spectra that may or may not fit a known template and in analyzing the region of the β-band. That of Lamb [19] derives its usefulness as a single function that extends through the crest of the α-band to long wavelengths where spectral sensitivity has fallen several log units from the wavelength of maximal sensitivity. Each of these formulations has its advantages, and both are an improvement over polynomial functions that require more coefficients and many more significant figures in order to achieve equivalent accuracy. Most importantly, a single template describes vertebrate rods [19], primate cones [44], and three retinal$_1$-based fish cones with λ_{max} in the visible region of the spectrum [10]. Narrower normalized-frequency templates are required for the UV cones of *Danio aequipinnatus* [10] and retinal$_1$-based amphibian rods [20].

Only Stavenga et al. [18] have tried to fit porphyropsin spectra to a template based on normalized frequency, but the template of Mooij and van den Berg [45] is notable for its effort to describe the long wavelength tail of absorption of retinal$_2$ visual pigments. Fig. 12 compares the template in Fig. 4 with these two earlier reports. When plotted as absorbance, the three templates are similar, and each can of course be no more accurate than the data from which it was constructed. That of Stavenga et al. [18] is based on a spectrum of porphyropsin from fish rods [24]; that of Mooij and van den Berg [45] on MSP measurements of goldfish cones [46]. The differences among the three are small, and confidence in the spectral shape can be expected to increase as the available data base enlarges.

Mooij and van den Berg [45] extended their template to long wavelengths by fitting goldfish ERG data to a modified form of a function first proposed by Lewis

[47] to account for the combined action of light and heat in the bleaching of rhodopsin. Their curves for three spectral classes of cone are compared with our retinal$_2$ template and the retinal$_1$ template of Lamb [19] (Fig. 13). Note that on a normalized frequency axis, the long-wavelength limbs of the Lamb-type retinal$_1$ and retinal$_2$ templates have very similar slopes (Table 4).

Acknowledgements

This work was supported by Grants EY-00222 and EY-00758 from the National Eye Institute and CEE grant ERBCHRXCT 930183. We thank Clint Makino for providing numerical data and further information on *Ambystoma* cones.

References

[1] Neumeyer C. Tetrachromatic color vision in goldfish: evidence from color mixture experiments. J Comp Physiol 1992;A171:639–49.
[2] Fratzer C, Dörr S, Neumeyer C. Wavelength discrimination of the goldfish in the ultraviolet spectral range. Vis Res 1994;34:1515–20.
[3] Bowmaker JK. The visual pigments of fish. Prog Retin Eye Res 1995;15:1–31.
[4] Stell WK, Hárosi FI. Cone structure and visual pigment content in the retina of the goldfish. Vis Res 1976;16:647–57.
[5] Marc RE, Sperling HG. The chromatic organization of the goldfish cone mosaic. Vis Res 1976;16:1211–24.
[6] Raymond PA, Barthel LK, Rounsifer ME, Sullivan SA, Knight JK. Expression of rod and cone visual pigments in goldfish and zebrafish: a rhodopsin-like gene is expressed in cones. Neuron 1993;10:1161–74.
[7] Hárosi FI, MacNichol EF Jr. Visual pigments of goldfish cones. J Gen Physiol 1974;63:279–304.
[8] Bowmaker JK, Thorpe A, Douglas RH. Ultraviolet-sensitive cones in the goldfish. Vis Res 1991;31:349–52.
[9] Hárosi FI. An analysis of two spectral properties of vertebrate visual pigments. Vis Res 1994;34:1359–67.
[10] Palacios AG, Goldsmith TH, Bernard GD. Sensitivity of cones from a cyprinid fish (*Danio aequipinnatus*) to ultraviolet and visible light. Vis Neurosci 1996;13:411–21.
[11] Johnson RL, Gran KB, Zankel TC, Boehm MF, Merbs SL, Nathans J, Nakanishi K. Cloning and expression of goldfish opsin sequences. Biochemistry 1993;32:208–14.
[12] Okano T, Kojima Y, Fukada Y, Schichida Y, Yoshizawa T. Primary structures of chicken cone visual pigments: vertebrate rhodopsins have evolved out of cone visual pigments. Proc Natl Acad Sci USA 1992;89:5932–6.
[13] Hisatomi O, Satoh T, Barthel LK, Stenkamp DL, Raymond PA, Tokunaga F. Molecular cloning and characterization of the putative ultraviolet-sensitive visual pigment of goldfish. Vis Res 1996;36:933–9.
[14] Dartnall HJA. The interpretation of spectral sensitivity curves. Br Med Bull 1953;9:24–30.
[15] Ebrey TG, Honig B. New wavelength dependent visual pigment nomograms. Vis Res 1977;17:147–51.
[16] Mansfield RJW. Primate photopigments and cone mechanisms. In: Fein A, Levine JS, editors. The Visual System. New York: Alan R Liss, 1985:89–106.
[17] MacNichol EFJr. A unifying presentation of photopigment spectra. Vis Res 1986;26:1543–56.
[18] Stavenga DA, Smits RP, Hoenders BJ. Simple exponential functions describing the absorbance bands of visual pigment spectra. Vis Res 1993;33:1011–7.
[19] Lamb TD. Photoreceptor spectral sensitivities: common shape in the long-wavelength region. Vis Res 1995;35:3083–91.
[20] Palacios AG, Srivastava R, Goldsmith TH. Spectral and polarization sensitivity of photocurrents of amphibian rods in the visible and ultraviolet. Vis Neurosci 1998;15:319–31.
[21] Palacios AG, Goldsmith TH. Spectral sensitivity of retinal cones in the goldfish (*Carassius auratus*). Soc Neurosci Abstr Annu Meet 1993;19:1200.
[22] Low JC, Yamada M, Djamgoz MBA. Voltage clamp study of electrophysiologically-identified horizontal cells in carp retina. Vis Res 1991;31:437–49.
[23] Baylor DA, Hodgkin AL. Detection and resolution of visual stimuli by turtle photoreceptors. J Physiol Lond 1973;234:163–98.
[24] Bridges CDB. The rhodopsin-porphyropsin visual system. In: Dartnall HJA, editor. Handbook of Sensory Physiology, VII/1, Photochemistry of Vision. Berlin: Springer-Verlag, 1972:471–80.
[25] Groenendijk GWT, DeGrip WJ, Daemen FJ. Quantitative determination of retinals with complete retention of their geometric configuration. Biochim Biophys Acta 1980;617:430–8.
[26] Goldsmith TH, Cronin TW. The retinoids of seven species of mantis shrimp. Vis Neurosci 1993;10:915–20.
[27] Perry RJ, McNaughton PA. Response properties of cones from retina of the tiger salamander. J Physiol Lond 1991;433:561–87.
[28] Miller JL, Korenbrot JI. Phototransduction and adaptation in rods, single cones, and twin cones of the striped bass retina: a comparative study. Vis Neurosci 1993;10:653–67.
[29] Lamb TD, McNaughton PA, Yau KW. Spatial spread of activation and background desensitization in toad rod outer segments. J Physiol Lond 1981;319:463–96.
[30] Naka KI, Rushton WAH. S-potentials from colour units in the retina of fish (*Cyprinidae*). J Physiol Lond 1966;185:536–55.
[31] Walls G. The Vertebrate Eye and its Adaptive Radiation. New York: Hafner, 1942.
[32] Engström K. Cone types and cone arrangements in teleost retinae. Acta Zool 1963;44:179–243.
[33] Makino CL, Dodd RL. Multiple visual pigments in a photoreceptor of the salamander retina. J Gen Physiol 1996;108:27–34.
[34] Chen DM, Stark WS. Electroretinographic analysis of ultraviolet sensitivity in juvenile and adult goldfish retinas. Vis Res 1994;34:2941–4.
[35] Bowmaker JK, Kunz YW. Ultraviolet receptors, tetrachromatic colour vision and retinal mosaics in the brown trout (*Salmo trutta*): age-dependent changes. Vis Res 1987;27:2101–8.
[36] Kunz YW, Wildenburg G, Goodrich L, Callaghan E. The fate of ultraviolet receptors in the retina of the Atlantic salmon (*Salmo salar*). Vis Res 1994;34:1375–83.
[37] Whitmore AV, Bowmaker JK. Seasonal variation in the core sensitivity and short-wave-absorbing visual pigments in the rudd *Scardinius erythrophthalmus*. J Comp Physiol A 1989;166:103–15.
[38] Kropf A. Intramolecular energy transfer in rhodopsin. Vis Res 1967;7:811–8.
[39] Tsin AT, Beatty DD. Goldfish rhodopsin: P499$_1$. Vis Res 1978;18:1453–5.
[40] Tsin AT, Liebman PA, Beatty DD, Drzymala R. Rod and cone visual pigments in the goldfish. Vis Res 1981;21:943–6.
[41] Beatty DD. Visual pigments and the labile scotopic visual system of fish. Vis Res 1984;24:1563–73.
[42] Wald G, Brown PK, Smith PH. Cyanopsin, a new pigment of cone vision. Science 1953;118:505–8.

[43] Tomita T, Kaneko A, Murakami M, Pautler EL. Spectral response curves of single cones in the carp. Vis Res 1967;7:519–31.
[44] Baylor DA, Nunn BJ, Schnapf JL. Spectral sensitivity of cones of the monkey *Macaca fascicularis*. J Physiol 1987;390:145–60.
[45] Mooij JE, van den Berg TJ. The spectral shape of A_2 visual pigments. Vis Res 1983;23:701–5.
[46] Hárosi FI. Spectral relations of cone pigments in goldfish. J Gen Physiol 1976;68:65–80.
[47] Lewis PR. A theoretical interpretation of spectral sensitivity curves at long wavelengths. J Physiol Lond 1955;130:45–52.
[48] Liebman PA, Entine G. Sensitive low-light-level microspectrophotometer: detection of photosensitive pigments of retinal cones. J Opt Soc Am 1964;54:1451–9.
[49] Liebman PA. Microspectrophotometry of photoreceptors. In: Dartnall HJA, editor. Handbook of Sensory Physiology, VII/1, Photochemistry of Vision. Berlin: Springer-Verlag, 1972:481–528.
[50] Marks WB. Visual pigments of single goldfish cones. J Physiol Lond 1965;178:14–32.
[51] Morton RA. The chemistry of visual pigments. In: Dartnall HJA, editor. Handbook of Sensory Physiology, VII/1, Photochemistry of Vision. Berlin: Springer-Verlag, 1972:33–68.